Sensors and actuators B: Chemical

Integrated platform for detecting pathogenic DNA via magnetic tunneling junction-based biosensors

DOI: 10.1016/j.snb.2016.11.051

Parikshit P. Sharma[a], Edoardo Albisetti[a], Matteo Massetti[a], Martina Scolari[a], Chiara La Torre[a], Marco Monticelli[a], Marco Leone[b], Francesco Damin[c], Giacomo Gervasoni[d], Giorgio Ferrari[d], Fabio Salice[e], Emanuele Cerquaglia[f], Giorgio Falduti[g], Marina Cretich[c], Edoardo Marchisio[g], Marcella Chiari[c], Marco Sampietro[d], Daniela Petti[a,*] and Riccardo Bertacco[a]

[a]Dipartimento di Fisica, Politecnico di Milano, Via Giuseppe Colombo 81, 20133 Milan, Italy
[b]L-NESS, Dipartimento di Fisica, Politecnico di Milano, Via Anzani 42, 22100 Como, Italy
[c]Istituto di Chimica del Riconoscimento Molecolare, CNR, Via Mario Bianco 9, 20131 Milan, Italy
[d]Dipartimento di Elettronica, Informazione e Bioingegneria, Politecnico di Milano, Via Giuseppe Colombo 81, 20133 Milan, Italy
[e]Dipartimento di Elettronica, Informazione e Bioingegneria, Politecnico di Milano, Via Anzani 42, 22100 Como, Italy
[f]Myti Tecnologie Informatiche srl, Via Branze 44, 25123, Brescia, Italy
[g]Dia.Pro Diagnostic BioProbes srl, Via Giosuè Carducci 27, 20099 Sesto San Giovanni, Italy

* Corresponding Author:
Daniela Petti,
daniela.petti@polimi.it
Dipartimento di Fisica - Politecnico di Milano
Via G. Colombo, 81 20133 Milano, Italy
Office +39 02 2399 9660

Abstract

In recent years, the development of portable platforms for performing fast and point-of-care analyses has drawn considerable attention for their wide variety of applications in life science. In this framework, tools combining magnetoresistive biosensors with magnetic markers have been widely studied in order to detect concentrations of specific molecules, demonstrating high sensitivity and ease of integration with conventional electronics. In this work, first, we develop a protocol for efficient hybridization of natural DNA; then, we show the detection of hybridization events involving natural DNA, namely genomic DNA extracted from the pathogenic bacterium *Listeria monocytogenes*, via a compact magnetic tunneling junction (MTJ)-based biosensing apparatus. The platform comprises dedicated portable electronics and microfluidic setups, enabling point-of-care biological assays. A sensitivity below the nM range is demonstrated. This work constitutes a step forward towards the development of portable lab-on-chip platforms, for the multiplexed detection of pathogenic health threats in food and food processing environment.

Keywords

Magnetic biosensor, Magnetic tunnelling junction, Magnetic bead, Genotyping, Listeria, Point-of-care.

1. Introduction

Waterborne and foodborne pathogens play a crucial role when dealing with health threats and public safety. Finding highly sensitive biological detection schemes, suitable for rapid and point-of-care assays, has therefore become an important technological challenge.

In this context, several kinds of biosensors have been proposed [1]. In particular, genosensor, i.e. sensors capable of detecting nucleic acids, are considered to be extremely promising [2–4]. They are mainly based on the natural affinity of single strand DNA (ssDNA) to its complementary strand, allowing the detection of specific target genes. DNA microarrays represent a widely used, fast and low cost implementation of this concept, exploiting the immobilization of different DNA probes on the same substrate to achieve multiplexing. The use of nucleic acid as recognition elements ensures long-term stability, high temperature resistance, and ease of chemical modification after the initial synthesis. The detection of biomolecular recognition is then achieved via several methods. Among others, we mention electrochemical transduction [5–7], fluorescence [8–10], chemiluminescence [11,12], surface plasmon resonance [13] and magnetoresistive (MR) detection [14,15]. The latter technology combines extremely low noise, because of the absence of magnetic background in most biological environments, with very high sensitivity. The most widespread detection scheme employs

MR sensors combined with magnetic markers. Molecular recognition takes place between probe molecules, bound onto the sensor surface, and magnetically labeled target molecules, which bind specifically to the complementary probes. The magnetic stray field of the superparamagnetic labels in proximity to the sensor surface causes a change in the electrical resistance of the sensor, which is related to the concentration of the immobilized target molecules. Giant magnetoresistive (GMR) sensors arrays based on spin-valves have been successfully used to detect synthetic DNA hybridization events and protein interactions with concentrations in the femto- to zepto-molar range [15–17]. MTJ-based sensors have been also employed for detecting magnetic particles at low concentrations [18,19] and synthetic DNA hybridization events [20–23].

Together with their high sensitivity, the ease of integration with conventional electronics makes the MR sensors among the most promising candidates for the development of compact platforms able to perform point-of-care (POC) detection, thus enabling fast on-site (OS) screening for pathogens.

One of the first works employing a MR sensor platform for the detection of magnetic nanoparticles was based on GMR sensors integrated in a disposable cartridge [24]. A MTJs array embedded in a microfluidic cartridge has been used for the detection of AMI bio-markers [25]. Two different MR handheld platforms, with portable electronics but without microfluidics, have been validated through synthetic DNA hybridization experiments [26] and washing-free immunoassays [27].

In this work, we accomplish a fundamental step towards the exploitation of MTJs based biosensors. We demonstrate the detection of natural DNA hybridization, in a real case of bacteria genotyping, utilizing a portable MTJ-based platform provided with electronic and microfluidic apparatus. One of the major issues, when dealing with natural DNA, is related to the length of the oligonucleotides (70/100-mer in our case), which leads to a reduced efficiency both in the hybridization and in the subsequent labelling, due to steric hindrance [28]. This problem was overcome by combining optimized hybridization and magnetic labelling protocols with highly sensitive MTJ-based biosensors.

The paper is organized as follows. First, we demonstrate the magnetic detection of hybridization events of natural DNA extracted from *Hepatitis E virus*, *Listeria monocytogenes* and *Salmonella typhimurium* bacteria. Then, we validate our portable MTJ-based platform (Fig. 1), detecting the DNA of *Listeria monocytogenes* with a sensitivity below the nM range. This work paves the way to the deployment of lab-on-chip platforms based on MTJs for point-of-care investigation of biological pathogenic threats in agrifood environment.

2. Materials and Methods

2.1 Sensor definition

The sensor stacks consist of a CoFeB/MgO/CoFeB MTJ, where the magnetization of the bottom layer is pinned by a synthetic antiferromagnet [29]. The multilayers were grown on Si/SiO_2 substrates by magnetron sputtering in an AJA Orion8 system with a base pressure of $2 \cdot 10^{-9}$ Torr and an applied magnetic field of 300 Oe [21,30]. The whole deposited stack is reported hereafter (thickness in nm): Ta(5)/ Ru(18)/ Ta(3)/ $Ir_{20}Mn_{80}$(20)/ $Co_{60}Fe_{40}$(1.8)/ Ru(0.9)/ $Co_{40}Fe_{40}B_{20}$(2.7)/ MgO(2.5)/ $Co_{40}Fe_{40}B_{20}$(1.3)/ Ru(5)/ Ta(20). $Co_{60}Fe_{40}$ and MgO layers were deposited in RF mode while the remaining layers were grown in DC mode.

After deposition, the stacks were processed with optical lithography and ion beam etching in order to obtain sensor chips featuring 12 MTJ sensors arrays (Fig. 1(c), Fig. 2(a)). The junction areas are 3 x 40 μm^2, with the shorter side parallel to the easy-axis of the bottom pinned layer. A 100 nm thick SiO_2 layer was deposited for insulating purposes. Afterwards, the Cr(7)/ Au(300) contact layers were deposited by electron beam evaporation. The sensors arrays were then annealed at 310°C at a pressure of 10^{-6} Torr for 1 hour; this step was performed to enable the crystallization of the ferromagnetic layers, thus promoting coherent tunneling [31,32]. A $SiO_2(50)/Si_3N_4(100)/SiO_2(70)$ trilayer was sputtered on the sensors for protecting them from the harsh biological environment. The sensor response to a magnetic field applied parallel to the shorter side of the junction area (Fig. 2(b)) is shown in Fig. 2(d), featuring a 45% MR ratio and a low-field sensitivity $S_o = (R\mu_0)^{-1}(dR/dH)$ = 13.6%/mT. The linearity and low hysteresis of the response curve is the result of both the shape anisotropy [33] and the superparamagnetic behaviour of the top free layer [34].

2.2 Surface functionalization and hybridization

The general scheme utilized for the assays is the "post-hybridization method" [35], in which the magnetic labeling takes place after the hybridization.

First, the chips were coated with a functional copolymer (DMA-NAS-MAPS) [36] in order to provide active ester moieties suitable for immobilization of amino modified oligonucleotides and, at the same time, prevent non-specific adsorption of biological fluids components. Copoly(DMA-NAS-MAPS) has been extensively used as a functional coating in DNA microarrays [37–41] and various biosensing applications [22,42,43] for its favorable characteristics in terms of simplicity of use, high probe binding capacity and excellent anti-fouling properties. The probe oligonucleotides (20 µM, from MWG Biotech AG Germany), complementary or uncorrelated to the target DNA strands and modified with an amino group for allowing the covalent binding to the polymer, were then spotted on the different sensors surface, so as to implement positive and control bioassays on the very same

chip. For this purpose, a non-contact microarray spotter SCENION sci-FLEXARRAYER S5 assembled with an 80 μm nozzle was used. Spot volume of each drop, temperature and humidity were 400 pL, 22°C and 50%, respectively, and the spotting buffer was a 150 mM phosphate buffer (pH 8.5) with 0.01% sucrose monolaurate. Subsequently, the surface was incubated overnight with a blocking buffer (ethanolamine, 50 mM in a Tris/HCl buffer 0.1 M, 50° C), in order to prevent nonspecific binding during the hybridization step [22].

Bacterial plasmids DNA, containing a highly conserved region representative of the four major genotypes of *Hepatitis E Virus* (*HEV*) and *L. monocytogenes hly* (*Listeriosin O* encoding gene), was isolated from transformed *E. coli* overnight cultures. A NucleoSpin DNA purification kit (Macherey-Nagel, Duren, Germany) was employed according to the manufacturer's recommendations [44,45]. DNA target concentrations were checked by agarose gel electrophoresis and SYBR® Safe DNA gel staining (Invitrogen, Oregon, USA).

Biotinylated target DNA was then amplified by means of PCR, and then incubated on the sample surface for enabling hybridization. The last process requires first the denaturation of the amplified DNA, i.e. the separation of the two single strands, at a temperature of 95° C, and then the hybridization at a temperature of 40° C, in order to ensure high specificity during the binding process.

2.3 Microfluidic apparatus

After DNA hybridization, the chip is inserted into an apparatus providing both fluidic and electrical access to the sensors for the detection experiments. The platform (Fig. 1(a)) comprises a disposable aluminum chip-holder, placed on a movable carrier in order to easily insert and remove the biochip. A click-on microfluidic Poly(methyl methacrylate) (PMMA) chamber is positioned on the top of the chip by means of a small micro-positioner (Fig. 1(c)). The chamber, designed in order to promote a laminar flow inside the channel and to ensure a reliable washing procedure during the experiment, has a 2.2 x 0.7 mm^2 section. The large chamber width allows reducing the effect of the wall on the flow profile, while the reduced channel height assures an effective removal of the unbound beads from the surface of the chip. A Polydimethylsiloxane (PDMS) gasket is used to seal the chamber. The flow-rate is controlled by a syringe pump system connected to the lateral microfluidic channels with variable section and inclination, designed to avoid any flow turbulence (see Supplementary Information).

The chip-holder is provided with a Peltier cell for temperature control, in order to enable the integration of further processes such as DNA hybridization (see Supplementary Information for preliminary experiments) or PCR inside the channel.

The electrical connection is provided through retractable tips embedded in the PMMA top cover (see the sketch of Fig. 1(b) and Supplementary Information. In order to apply an external magnetic field, a low-remanence compact electromagnet is used (see Supplementary Information), able to generate a uniform magnetic field on the whole chip area.

2.4 Electronic setup and measurement configuration

A portable electronic platform was developed and connected to the apparatus described above. The platform comprises a digital module combining a Field Programmable Gate Array (FPGA) and a Hard Processor System (HPS), which is used to control the Peltier cell, the syringe pump, the electromagnet and the front-end electronics (see Supplementary Information). Two generation channels featuring a 16-bit resistor ladder DAC are employed to force a current in the magnetoresistive sensor and, through an analog power amplifier, for driving the electromagnet.

The voltage across the sensor is read and processed using a compact and low-noise lock-in amplifier [46]. A single acquisition chain has been implemented in order to simplify the architecture and limit power consumption. An input multiplexer selects one sensor at a time for the duration needed to perform low-pass filtering, i.e. about 1 s per sensor (configurable). Due to the limited number of sensors, the time required to complete an acquisition is well below the typical time of the bioassay, allowing a real-time monitoring of the experiment. After analog amplification and anti-aliasing filtering, the signal is converted with a 16-bit 1 Msps ADC. Then, demodulation and low-pass filtering are digitally performed on board and the measurement results are transferred to the PC. A dedicated software for the control of the platform was developed.

The general scheme utilized for the detection is the following: first, the chip comprising 12 sensors is functionalized in order to have 6 sensors and 6 controls. After the hybridization with complementary target DNA, the chip is integrated in the microfluidic cell. Then, the magnetic markers (Micromod® Nanomag®-D, 250 nm diameter streptavidin coated magnetic beads (75–80% (w/w) magnetite in a matrix of dextran (40 kD)), are dispersed in phosphate buffer (PB)-Tween solution (~10^8 particles/µl) and injected into the microfluidic cell at a flow rate of 50 µl/min. The flow is then stopped in order to let the beads settle down and interact with the biotinylated DNA immobilized on the sensor surface, while recording the sensor signal. Finally, with the washing step, the unbound beads are flushed away. The optical images of the sensors before and after the experiment are presented in Fig. 2(c), showing the beads immobilized on top of the sensors, in the spotted regions. During the measurement, an external magnetic field is applied parallel to the sensing axis in order to magnetize the beads and bias the sensor in its most sensitive point [21] and the sensors

signal is acquired in real-time. The microfluidic cell prevents the liquid evaporation thus allowing for a reliable monitoring of the different steps: sedimentation, hybridization and washing. In order to enhance the sensitivity and minimize the 1/f noise figure, a double modulation technique is used, i.e. both the junction voltage and the external magnetic field are modulated [21] at f_1=1.1 kHz and f_2 = 39 Hz, respectively. The magnetic signal, eventually depending on the concentration of beads above the sensor, appears in the output voltage (V_{out}) as a component at the frequency ($f_1 \pm f_2$), which is then extracted via the lock-in amplifier.

3. Results

3.1 Hybridization and labelling of natural DNA

Before employing the magnetic biosensing platform, standard fluorescence-based assays for testing the DNA hybridization efficiency, as well as for checking the non-specific binding of target DNA with non-complementary DNA probe, were performed.

Fig. 3 shows the results of three different fluorescence assays for *Listeria* (panel (a)), *HEV* (panel (b)) and *Salmonella* (panel (c)). In each assay, the complementary probe DNA and the control probe DNA were immobilized on spatially separated areas of the polymer-coated chip by micro-spotting. Then, hybridization with biotinylated target DNA, extracted from *Listeria* (70-mer target, panel (a)), *HEV* (100-mer target, panel (b)) and *Salmonella* (70-mer target, panel (c)), was carried out following the procedure described above. Subsequently, binding of fluorescent streptavidin (Cy3 dye) to the immobilized biotinylated target DNA was carried out. The high contrast of the bright spots, related to the concentration of hybridized complementary target DNA, confirms the efficiency of the immobilization and hybridization procedure. Moreover, the absence of contrast in the control area allows concluding that the non-specific binding of target DNA to non-complementary probes is low. This last feature is crucial in a prospect of implementing a multiplexed platform for the simultaneous detection of different pathogens. Finally, it is worth to notice that the same experiments, performed without probes immobilization, resulted in absence of contrast as well, suggesting that the polymeric coating is effective in preventing non-specific target DNA immobilization.

Preliminary experiments demonstrating the magnetic detection of hybridization of *HEV* and *Listeria* DNA were performed employing the non-integrated platform and measurement configurations of [20–22]. For the detection, each biochip was functionalized as described above, i.e. half of the sensors with the complementary probe and half (control sensors) with non-complementary probes. The control sensors are used to monitor the efficiency of the washing step. When the control signal returns

to the baseline, the removing of the unbound beads can be considered concluded. In Fig. 4, the results of the detection experiments of 100 nM *HEV* target DNA and 500 nM *Listeria* target DNA, are shown. In panel (a), the signal recorded from the sensor functionalized with *HEV* probe is shown as a function of time. Before bead injection, for $t < 1900$ s, the signal baseline is acquired; then, the solution with the beads is injected at $t = 1900$ s, and the nanoparticles are let to sedimentate onto the sensor surface for around 25 minutes, in order to allow the biotin-streptavidin binding. At $t = 3400$ s the washing solution (PB-Tween solution) is injected for removing the unbound beads from the surface of the sensors. The ΔS_H binding signal in panel (a) is related to the concentration of beads immobilized on the sensor after washing, due to the streptavidin-biotin interaction with the hybridized target DNA. The signal recorded from the control sensor, functionalized with *Klebsiella* probe, is shown in the Supplementary Information.

The low non-specific binding is confirmed by the absence of binding signal, as reported in the Supplementary Information, where the signal recovers the baseline after washing. The top part of Fig. 4(a) displays the optical image of the sensor area after the washing step, showing the magnetic markers specifically bound to the hybridized DNA. In Fig. 4(b), the results of the detection experiments of a chip hybridized with *Listeria* target DNA at a concentration of 500 nM are shown. The experiment was run in the same configuration as described above. Similarly, the ΔS_H binding signal is present only in the sensor functionalized with *Listeria* probe, and is absent in the control sensor (see Supplementary Information).

3.2 Listeria detection with the portable platform

Finally, experiments employing the fully integrated setup shown in Fig. 1 were performed. Hybridization detection experiments were performed on different chips, with *Listeria* target DNA at concentrations ranging from 1 µM to 1 nM. Each chip, comprising 12 MTJ sensors, was functionalized in order to have 6 sensors with specific probes and 6 control sensors with uncorrelated DNA sequences. The hybridization with complementary target DNA was performed outside the cell as described in paragraph 2.2. The experimental results are shown in Fig. 5 in case of 1 µM target concentration (panel (a)), and in case of 1 nM target concentration (panel (b)). Similarly to the previous cases, the ΔS_H binding signal is present only in the sensors functionalized with *Listeria* probe, and is absent in the control sensors, where the signal baseline is recovered after washing (see Supplementary Information and right graph in panel (b)). The optical image of the sensor area, acquired after the washing step, is shown in panel (a). As expected, the magnetic beads are immobilized on the sensor surface via biotin-streptavidin binding.

4. Discussion

From the sensor output, it is possible to determine the normalized binding signal ($\Delta S_H/\Delta S$, see Fig. 5), which is related to the target DNA concentration. $\Delta S_H/\Delta S$ is calculated considering the mean values of the baseline measured before and after the beads sedimentation, and after the washing step. The mean is calculated over about 250 values, acquired during the stabilization of all the baselines.

The $\Delta S_H/\Delta S$ obtained with the integrated platform are 0.81 ± 0.02 and 0.41 ± 0.11 in the experiments involving 1 µM and 1 nM concentration of *Listeria* target DNA, respectively. The values reported above are the mean values of the signals arising from different sensors acquired sequentially on the same chip. The error, in this case, is the standard deviation of these different measurements, arising mainly from the variability of the position of the spotted probes with respect to the sensor [22].

Several factors may influence the output signals, such as the binding efficiency of the biological probes [22], the quality of the washing step and the disturbances originating from the electronic setup [47]. In order to properly discriminate "false-positives" and "false-negatives", we assume that the confidence area corresponds to normalized binding signals on sensors at least three times higher than the spurious normalized binding signal on control sensors (S_{NC}). The latter defines the limit of sensitivity of the biosensing platform, and constitutes a relevant figure of merit for practical use.

In our case, the experimental value of S_{NC} is 0.060 ± 0.005, where the error is given by the standard deviation of the values measured on different control sensors. This variability arises from slightly different washing conditions and from the differences among the sensors due to the fabrication process, which reflects in slightly different hysteretic behaviours [33].

In both cases (1 µM and 1 nM target concentration), the normalized binding signal is well above the spurious normalized signal on control sensors (S_{NC}), so as to respect the above criterion of the confidence area, which is, in the worst case, $3^* S_{NC} = 0.20$.

In order to understand the impact of the integrated measurement apparatus on the sensitivity of our bioassay, we evaluate the uncertainty in the measurement introduced by the acquisition setup as the standard deviation of the baseline of the sensors normalized to the sedimentation signal ΔS (see Supplementary Information). This figure, namely the noise to signal ratio (NSR) is 0.02 and 0.06 for the experiments performed with 1 µM and 1 nM concentrations, respectively. The difference in the NSR of the two assays must be ascribed to sensor non-idealities arising from the fabrication process, such as variations in the barrier thickness [48], giving rise to different values of resistivity and thus to a different noise figure.

It is worth noting that uncertainty due to the integrated measurement setup are comparable with the sensitivity of the assays, i.e. 0.060 ± 0.005, thus allowing to conclude that the noise related to the integrated platform does not represent a major limitation for these specific biosensing purpose. We

can therefore conclude that that sensitivities below the nM range can be reached in case of natural DNA (see also Supplementary Information). Note that these results are comparable with or even better than those obtained in the case of *Listeria* genosensing with electrochemical biosensors [3,4].

5. Conclusions

In this work, we demonstrated the detection of natural DNA from pathogenic bacteria, using a highly sensitive biosensing platform based on magnetic tunneling junctions. First, assays for the detection of natural DNA extracted from *HEV*, *Listeria* and *Salmonella* were developed and tested via conventional fluorescence, and subsequently validated with the magnetic platform. In this framework, an effective protocol for the sensor functionalization, hybridization and labelling with magnetic markers was developed, resulting in a high selectivity and specificity. It is worth noting, that the orthogonality of the DNA probes allows to envision multiplexed assays, where the presence of multiple pathogens is assessed simultaneously in a single assay.

Finally, we realized a compact, integrated MTJ-based platform comprising dedicated electronics and microfluidics, for bacteria and viruses genotyping. As a proof-of-concept, we employed it for detecting different concentrations of DNA extracted from *Listeria bacterium*, demonstrating a sensitivity below the nanomolar range.

Thanks to its high sensitivity and specificity, the platform paves the way to the development of a multiplexed lab-on-chip apparatus for the point-of-care detection of pathogenic health threats.

Acknowledgments

The authors thank E-lysis (Roberto Galli, Roberto Mariani, Carlo Moroni) for their support in the development of the electronic platform, Alberto Salvati for the development of the software and Andrea Fogliani for the FEMM simulations.

This work was partially funded by MIUR-Regione Lombardia through the project Locsens (30071637). P.P.S., E.A., M.M. and D.P. acknowledge support from the Cariplo project UMANA (Project No. 2013-0735). M.S. and R.B. acknowledge support from Fondazione Cariplo and Regione Lombardia via the project Eschilo (2013-1760). This work was partially performed at Polifab, the micro-nano-fabrication facility of Politecnico di Milano.

Appendix A. Supplementary data

Supplementary data associated with this article can be found, in the online version, at [].

References

1. Lafleur, J. P.; Jönsson, A.; Senkbeil, S.; Kutter, J. P. Recent advances in lab-on-a-chip for biosensing applications. *Biosens. Bioelectron.* **2016**, *76*, 213–233.

2. Paniel, N.; Baudart, J.; Hayat, A.; Barthelmebs, L. Aptasensor and genosensor methods for detection of microbes in real world samples. *Methods* **2013**, *64*, 229–240.

3. Gupta, K.; Gupta, S.; Dubey, S. K.; Prakash, R. Genosensor based on Nanostructured Platinum Modified Glassy Carbon Electrode for *Listeria* Detection. *Anal. Methods* **2015**, *7*, 2616–2622.

4. Liébana, S.; Brandão, D.; Cortés, P.; Campoy, S.; Alegret, S.; Pividori, M. I. Electrochemical genosensing of *Salmonella*, *Listeria* and *Escherichia coli* on silica magnetic particles. *Anal. Chim. Acta* **2016**, *904*, 1–9.

5. Ölcer, Z.; Esen, E.; Ersoy, A.; Budak, S.; Sever Kaya, D.; Gök, M. Y.; Barut, S.; Üstek, D.; Uludag, Y. Microfluidics and nanoparticles based amperometric biosensor for the detection of cyanobacteria (*Planktothrix agardhii* NIVA-CYA 116) DNA. *Biosens. Bioelectron.* **2015**, *70*, 426–432.

6. Malecka, K.; Stachyra, A.; Góra-Sochacka, A.; Sirko, A.; Zagórski-Ostoja, W.; Radecka, H.; Radecki, J. Electrochemical genosensor based on disc and screen printed gold electrodes for detection of specific DNA and RNA sequences derived from *Avian Influenza Virus* H5N1. *Sensors Actuators B Chem.* **2016**, *224*, 290–297.

7. Korri-Youssoufi, H.; Miodek, A.; Ghattas, W. Electrochemical DNA Biosensors for Bioterrorism Prevention. In; Springer International Publishing, 2016; pp. 161–180.

8. Manesse, M.; Phillips, A. F.; LaFratta, C. N.; Palacios, M. a; Hayman, R. B.; Walt, D. R. Dynamic microbead arrays for biosensing applications. *Lab Chip* **2013**, *13*, 2153–60.

9. Liu, Z.; Su, X. A novel fluorescent DNA sensor for ultrasensitive detection of *Helicobacter pylori*. *Biosens. Bioelectron.* **2016**, *87*, 66–72.

10. Peltomaa, R.; Vaghini, S.; Patiño, B.; Benito-Peña, E.; Moreno-Bondi, M. C. Species-specific optical genosensors for the detection of mycotoxigenic *Fusarium fungi* in food samples. *Anal. Chim. Acta* **2016**, *935*, 231–238.

11. Liu, F.; Zhang, C. A novel paper-based microfluidic enhanced chemiluminescence biosensor for facile, reliable and highly-sensitive gene detection of *Listeria monocytogenes*. *Sensors Actuators, B Chem.* **2015**, *209*, 399–406.

12. Liu, M.; Li, B. Detection of DNA hybridization using a cationic polyfluorene polymer as an enhancer of luminol chemiluminescence. *Microchim. Acta* **2016**, *183*, 897–903.

13. Ghrera, A. S.; Pandey, M. K.; Malhotra, B. D. Quantum dot monolayer for surface plasmon resonance signal enhancement and DNA hybridization detection. *Biosens. Bioelectron.* **2016**, *80*, 477–482.

14. Zhi, X.; Deng, M.; Yang, H.; Gao, G.; Wang, K.; Fu, H.; Zhang, Y.; Chen, D.; Cui, D. A novel HBV genotypes detecting system combined with microfluidic chip, loop-mediated isothermal amplification and GMR sensors. *Biosens.*

Bioelectron. **2014**, *54*, 372–377.

15. Ng, E.; Nadeau, K. C.; Wang, S. X. Giant magnetoresistive sensor array for sensitive and specific multiplexed food allergen detection. *Biosens. Bioelectron.* **2016**, *80*, 359–365.

16. Martins, V. C.; Cardoso, F. a; Germano, J.; Cardoso, S.; Sousa, L.; Piedade, M.; Freitas, P. P.; Fonseca, L. P. Femtomolar limit of detection with a magnetoresistive biochip. *Biosens. Bioelectron.* **2009**, *24*, 2690–5.

17. Gaster, R. S.; Xu, L.; Han, S.-J.; Wilson, R. J.; Hall, D. a; Osterfeld, S. J.; Yu, H.; Wang, S. X. Quantification of protein interactions and solution transport using high-density GMR sensor arrays. *Nat. Nanotechnol.* **2011**, *6*, 314–20.

18. Donolato, M.; Sogne, E.; Dalslet, B. T.; Cantoni, M.; Petti, D.; Cao, J.; Cardoso, F.; Cardoso, S.; Freitas, P. P.; Hansen, M. F.; Bertacco, R. On-chip measurement of the Brownian relaxation frequency of magnetic beads using magnetic tunneling junctions. *Appl. Phys. Lett.* **2011**, *98*, 073702.

19. Shen, W.; Liu, X.; Mazumdar, D.; Xiao, G. In situ detection of single micron-sized magnetic beads using magnetic tunnel junction sensors. *Appl. Phys. Lett.* **2005**, *86*, 253901.

20. Albisetti, E.; Petti, D.; Damin, F.; Cretich, M.; Bagnati, M.; Sola, L.; Chiari, M.; Bertacco, R. Optimization of the bio-functionalized area of magnetic biosensors. *Eur. Phys. J. B* **2013**, *86*, 261.

21. Albisetti, E.; Petti, D.; Cantoni, M.; Damin, F.; Torti, a; Chiari, M.; Bertacco, R. Conditions for efficient on-chip magnetic bead detection via magnetoresistive sensors. *Biosens. Bioelectron.* **2013**, *47*, 213–7.

22. Albisetti, E.; Petti, D.; Damin, F.; Cretich, M.; Torti, a.; Chiari, M.; Bertacco, R. Photolithographic bio-patterning of magnetic sensors for biomolecular recognition. *Sensors Actuators B Chem.* **2014**, *200*, 39–46.

23. Shen, W.; Schrag, B. D.; Carter, M. J.; Xiao, G. Quantitative detection of DNA labeled with magnetic nanoparticles using arrays of MgO-based magnetic tunnel junction sensors. *Appl. Phys. Lett.* **2008**, *93*, 033903.

24. de Boer, B. M.; Kahlman, J. a H. M.; Jansen, T. P. G. H.; Duric, H.; Veen, J. An integrated and sensitive detection platform for magneto-resistive biosensors. *Biosens. Bioelectron.* **2007**, *22*, 2366–70.

25. Lian, J.; Chen, S.; Qiu, Y.; Zhang, S.; Shi, S.; Gao, Y. A fully automated in vitro diagnostic system based on magnetic tunnel junction arrays and superparamagnetic particles. *J. Appl. Phys.* **2012**, *111*, 10–13.

26. Germano, J.; Martins, V. C.; Cardoso, F. A.; Almeida, T. M.; Sousa, L.; Freitas, P. P.; Piedade, M. S. A portable and autonomous magnetic detection platform for biosensing. *Sensors* **2009**, *9*, 4119–4137.

27. Gaster, R. S.; Hall, D. a; Wang, S. X. nanoLAB: an ultraportable, handheld diagnostic laboratory for global health. *Lab Chip* **2011**, *11*, 950–6.

28. Southern, E.; Mir, K.; Shchepinov, M. Molecular interactions on microarrays. *Nat. Genet.* **1999**, *21*, 5–9.

29. Sharma, P. P.; Albisetti, E.; Monticelli, M.; Bertacco, R.; Petti, D. Exchange bias tuning for magnetoresistive sensors by inclusion of non-magnetic impurities. *Sensors (Switzerland)* **2016**, *16*, 1030.

30. Petti, D. Magnetic Tunneling Junctions for biosensors : form the growth to the detection. *Nuovo Cim. C* **2012**, *35*,

149–156.

31. Yuasa, S.; Djayaprawira, D. D. Giant tunnel magnetoresistance in magnetic tunnel junctions with a crystalline MgO(0 0 1) barrier. *J. Phys. D. Appl. Phys.* **2007**, *40*, R337–R354.

32. Petti, D.; Albisetti, E.; Reichlová, H.; Gazquez, J.; Varela, M.; Molina-Ruiz, M.; Lopeandía, a. F.; Olejník, K.; Novák, V.; Fina, I.; Dkhil, B.; Hayakawa, J.; Marti, X.; Wunderlich, J.; Jungwirth, T.; Bertacco, R. Storing magnetic information in IrMn/MgO/Ta tunnel junctions via field-cooling. *Appl. Phys. Lett.* **2013**, *102*, 192404.

33. Lu, Y.; Altman, R. a.; Marley, a.; Rishton, S. a.; Trouilloud, P. L.; Xiao, G.; Gallagher, W. J.; Parkin, S. S. P. Shape-anisotropy-controlled magnetoresistive response in magnetic tunnel junctions. *Appl. Phys. Lett.* **1997**, *70*, 2610.

34. Wiśniowski, P.; Almeida, J. M.; Cardoso, S.; Barradas, N. P.; Freitas, P. P. Effect of free layer thickness and shape anisotropy on the transfer curves of MgO magnetic tunnel junctions. *J. Appl. Phys.* **2008**, *103*, 07A910.

35. Baselt, D. R.; Lee, G. U.; Natesan, M.; Metzger, S. W.; Sheehan, P. E.; Colton, R. J. A biosensor based on magnetoresistance technology. *Biosens. Bioelectron.* **1998**, *13*, 731–9.

36. Pirri, G.; Damin, F.; Chiari, M.; Bontempi, E.; Depero, L. E. Characterization of A Polymeric Adsorbed Coating for DNA Microarray Glass Slides. *Anal. Chem.* **2004**, *76*, 1352–1358.

37. Cretich, M.; Sedini, V.; Damin, F.; Pelliccia, M.; Sola, L.; Chiari, M. Coating of nitrocellulose for colorimetric DNA microarrays. *Anal. Biochem.* **2010**, *397*, 84–88.

38. Yalçın, A.; Damin, F.; Özkumur, E.; di Carlo, G.; Goldberg, B. B.; Chiari, M.; Ünlü, M. S. Direct Observation of Conformation of a Polymeric Coating with Implications in Microarray Applications. *Anal. Chem.* **2009**, *81*, 625–630.

39. Özkumur, E.; Yalçın, A.; Cretich, M.; Lopez, C. A.; Bergstein, D. A.; Goldberg, B. B.; Chiari, M.; Ünlü, M. S. Quantification of DNA and protein adsorption by optical phase shift. *Biosens. Bioelectron.* **2009**, *25*, 167–172.

40. Petti, D.; Torti, A.; Damin, F.; Sola, L.; Rusnati, M.; Albisetti, E.; Bugatti, A.; Bertacco, R.; Chiari, M. Functionalization of gold surfaces with copoly(DMA-NAS-MAPS) by dip coating: Surface characterization and hybridization tests. *Sensors Actuators B Chem.* **2014**, *190*, 234–242.

41. Cretich, M.; Sedini, V.; Damin, F.; Di Carlo, G.; Oldani, C.; Chiari, M. Functionalization of poly(dimethylsiloxane) by chemisorption of copolymers: DNA microarrays for pathogen detection. *Sensors Actuators B Chem.* **2008**, *132*, 258–264.

42. Oliviero, G.; Bergese, P.; Canavese, G.; Chiari, M.; Colombi, P.; Cretich, M.; Damin, F.; Fiorilli, S.; Marasso, S. L.; Ricciardi, C.; Rivolo, P.; Depero, L. E. A biofunctional polymeric coating for microcantilever molecular recognition. *Anal. Chim. Acta* **2008**, *630*, 161–167.

43. Platt, G. W.; Damin, F.; Swann, M. J.; Metton, I.; Skorski, G.; Cretich, M.; Chiari, M. Allergen immobilisation and signal amplification by quantum dots for use in a biosensor assay of IgE in serum. *Biosens. Bioelectron.* **2014**, *52*, 82–8.

44. Rodríguez-Lázaro, D.; Hernández, M.; Scortti, M.; Esteve, T.; Vázquez-Boland, J.; Pla, M. Quantitative detection of Listeria monocytogenes and Listeria innocua by real-time PCR: assessment of hly, iap, and lin02483 targets and

AmpliFluor technology. *Appl Env. Microbiol* **2004**, *70*, 1366–1377.

45. Enouf, V.; Dos Reis, G.; Guthmann, J. P.; Guerin, P. J.; Caron, M.; Marechal, V.; Nicand, E. Validation of single real-time TaqMan PCR assay for the detection and quantitation of four major genotypes of hepatitis E virus in clinical specimens. *J. Med. Virol.* **2006**, *78*, 1076–1082.

46. Gervasoni, G.; Carminati, M.; Ferrari, G.; Albisetti, E.; Petti, D.; Sharma, P. P.; Bertacco, R.; Sampietro, M. A 12-channel dual-lock-in platform for magneto-resistive DNA detection with ppm resolution. *Biomed. Circuits Syst. Conf.* **2014**, 316–319.

47. Almeida, J. M.; Ferreira, R.; Freitas, P. P.; Langer, J.; Ocker, B.; Maass, W. 1/*f* noise in linearized low resistance MgO magnetic tunnel junctions. *J. Appl. Phys.* **2006**, *99*, 08B314.

48. Hayakawa, J.; Ikeda, S.; Matsukura, F.; Takahashi, H.; Ohno, H. Dependence of giant tunnel magnetoresistance of sputtered CoFeB/MgO/CoFeB magnetic tunnel junctions on MgO barrier thickness and annealing temperature. *Japanese J. Appl. Physics, Part 2 Lett.* **2005**, *44*, 2–5.

Captions

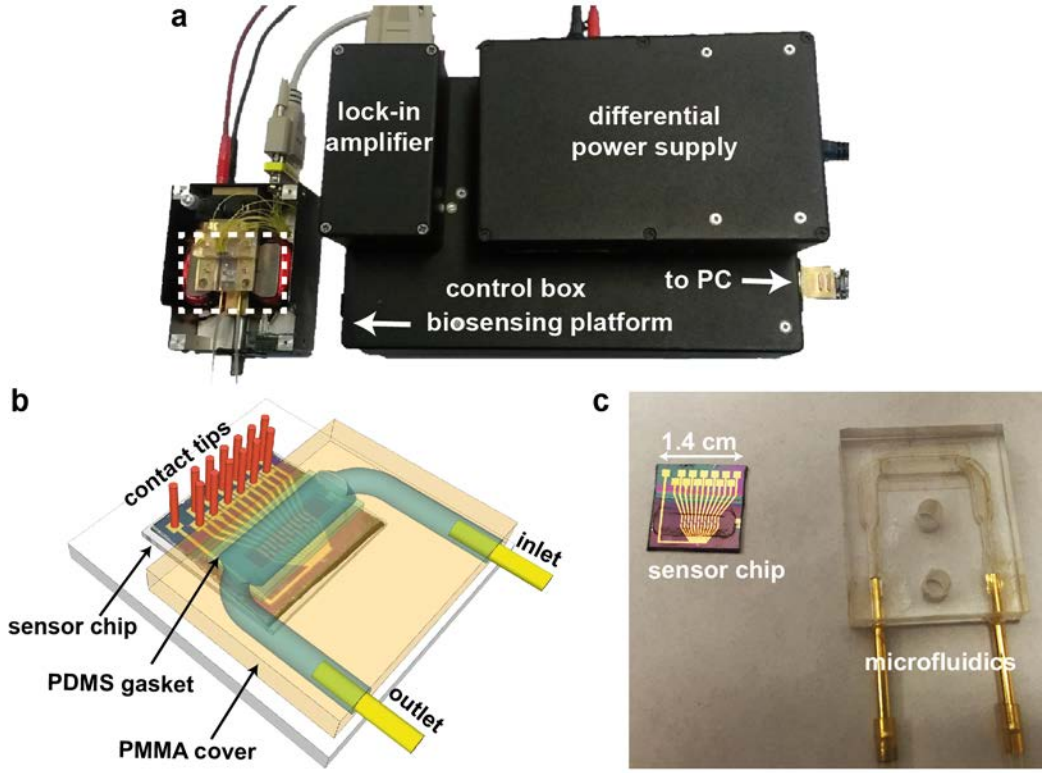

Fig. 1. (Color online) (a). Picture of the biosensing setup comprising the biosensing platform, the integrated lock-in amplifier, the control box for signal generation/acquisition and power supply. The microfluidic apparatus, marked by the white dashed rectangle, is placed within the poles of a compact electromagnet. (b). Sketch of the microfabricated sensor array, integrated within the microfluidic apparatus. Inlet and outlet fluidic channels are milled within the PMMA cover, and a PDMS gasket defines the chamber volume. Contact tips are used to independently address each MTJ-based sensor. (c). Picture of the sensor chip and microfluidic cell.

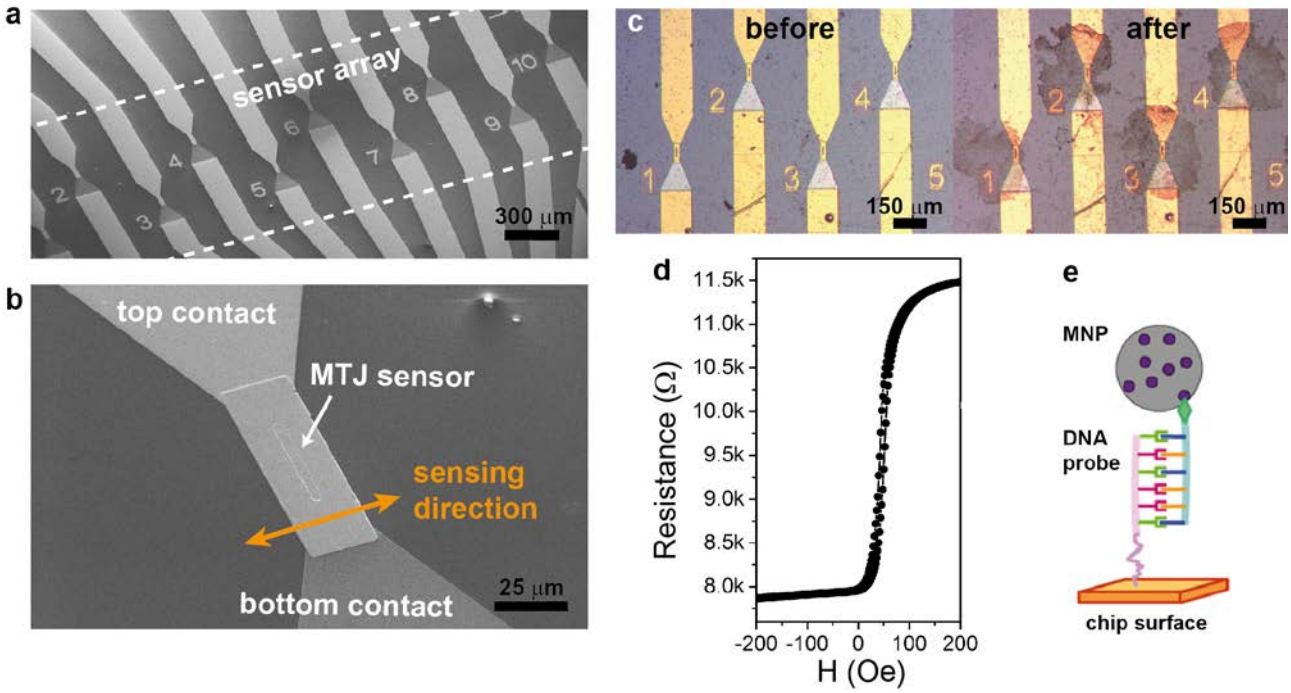

Fig. 2. (Color online) (a). SEM images of the sensor array comprising 12 MTJs with a common ground contact. (b). Zoomed view on a single MTJ sensor with a 40 x 3 μm^2 area. (c). Optical image of the sensor before and after the detection of 100 nM target *Listeria* DNA. (d). Magnetoresistive response curve of a sensor, measured along the sensing direction, featuring a 45% TMR ratio and 13.6%/mT low-field sensitivity. (e). Detection scheme with magnetic nanoparticles: streptavidinated magnetic markers are bound to the biotinilated natural target DNA, immobilized on the sensor surface via hybridization with complementary probe DNA.

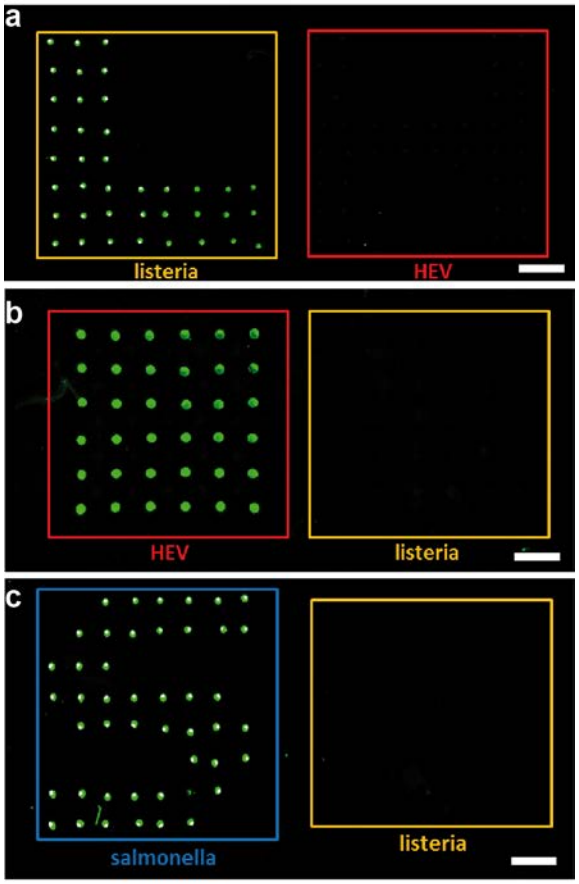

Fig. 3. (Color online) Fluorescence images of natural target DNA extracted from *Listeria monocytogenes*, left square in (a), *Hepatitis-E virus (HEV)*, left square in (b), *Salmonella typhimurium*, left square in (c), immobilized on the chip surface via hybridization with micro-spotted complementary probe DNA. The orthogonality of the DNA probes was confirmed by the low non-specific binding of *Listeria* target with *HEV* probe (right square in (a)), of *HEV* target with *Listeria* probe (right square in (b)), and of *Salmonella* target with *Listeria* probe (right square in (c)).

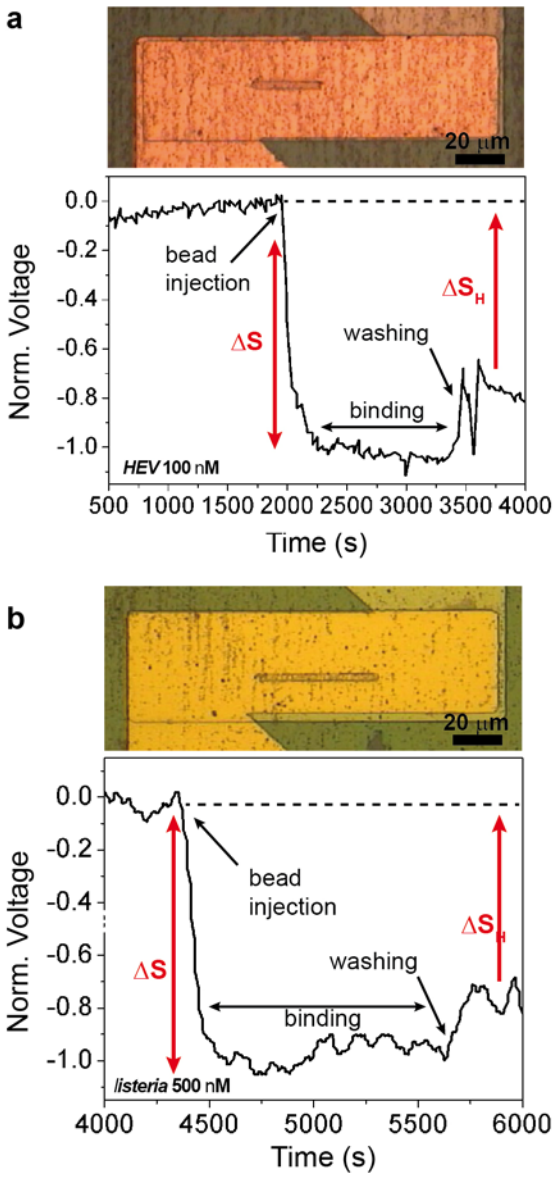

Fig. 4. (Color online) Validation of MTJ-based detection of hybridization of natural DNA. (a). In the bottom panel, normalized signal acquired as a function of time from a sensor functionalized with *HEV* probe, hybridized with 100 nM *HEV* target DNA. The sedimentation signal ΔS and the hybridization signal ΔS_H are indicated by red arrows. In the top panel, optical image of the sensor area after bead immobilization. (b). The same as in (a), from a sensor functionalized with *Listeria* probe, hybridized with 500 nM *Listeria* target DNA.

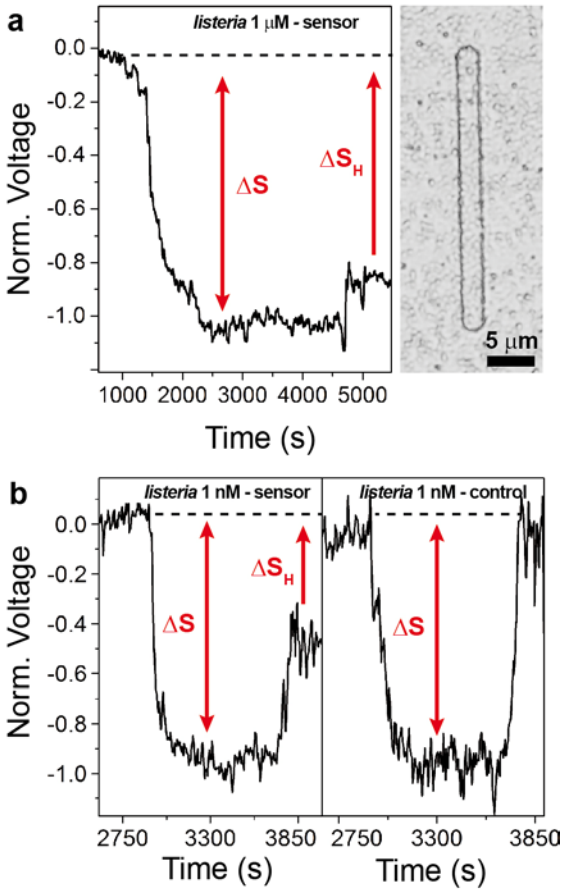

Fig. 5 (Color online) Detection of hybridization of natural DNA with the integrated platform. (a). Normalized signal acquired as a function of time from a sensor functionalized with *Listeria* probe, hybridized with 1 μM *Listeria* target DNA. The sedimentation signal ΔS and the hybridization signal ΔS_H are indicated by red arrows. In the right panel, optical image of the sensor area before the experiment and after bead immobilization. (b). In the left panel, normalized signal acquired as a function of time from a sensor functionalized with *Listeria* probe, hybridized with 1 nM *Listeria* target DNA. In the right panel, the signal from a control sensor, functionalized with *Klebsiella* probe, recovers the baseline after washing.